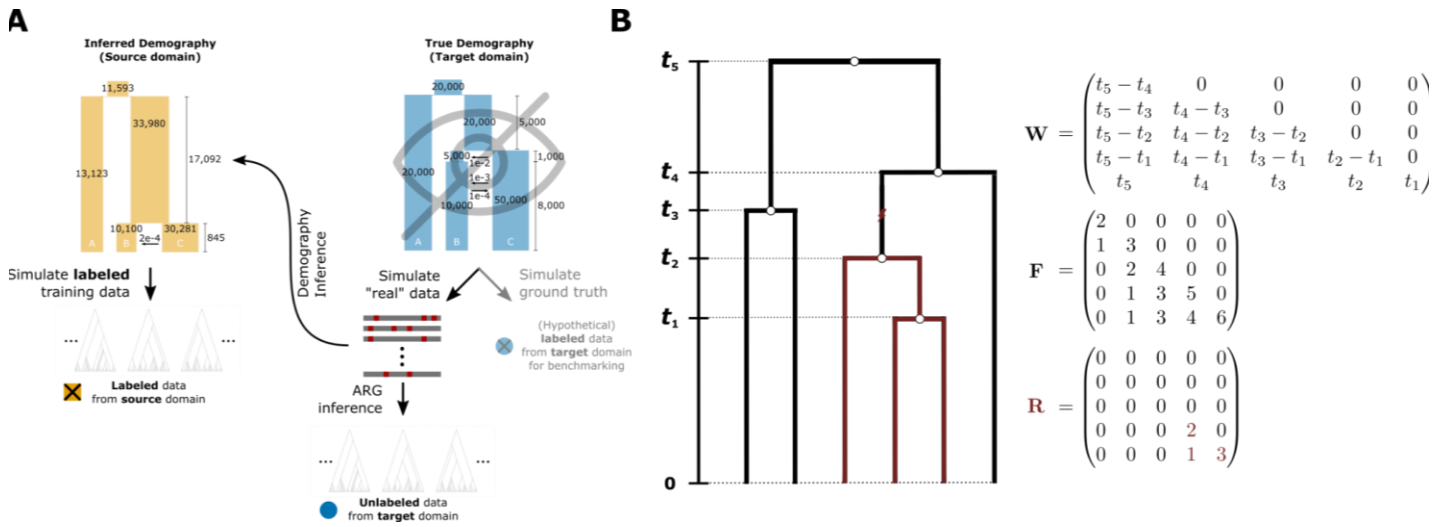
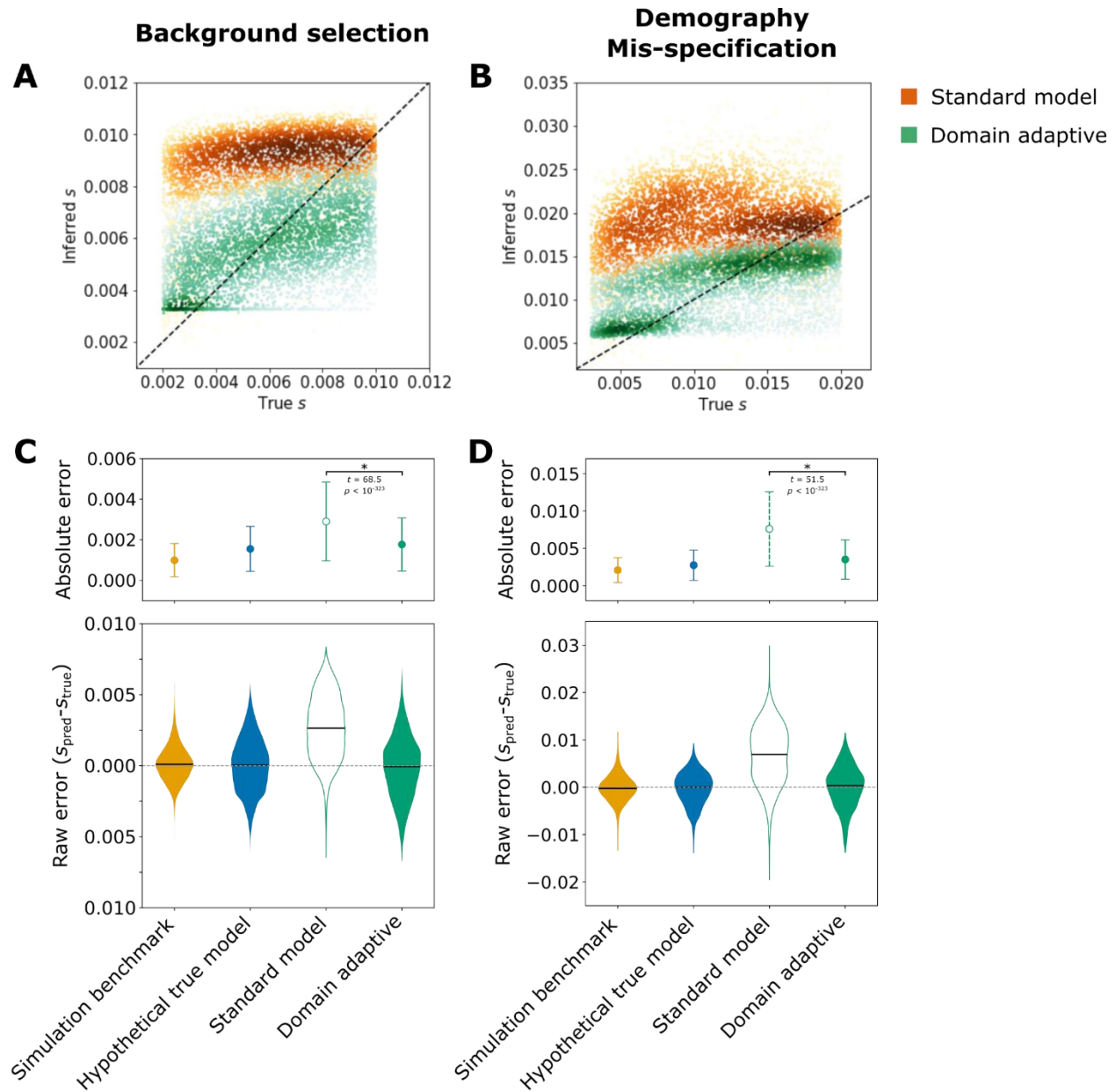


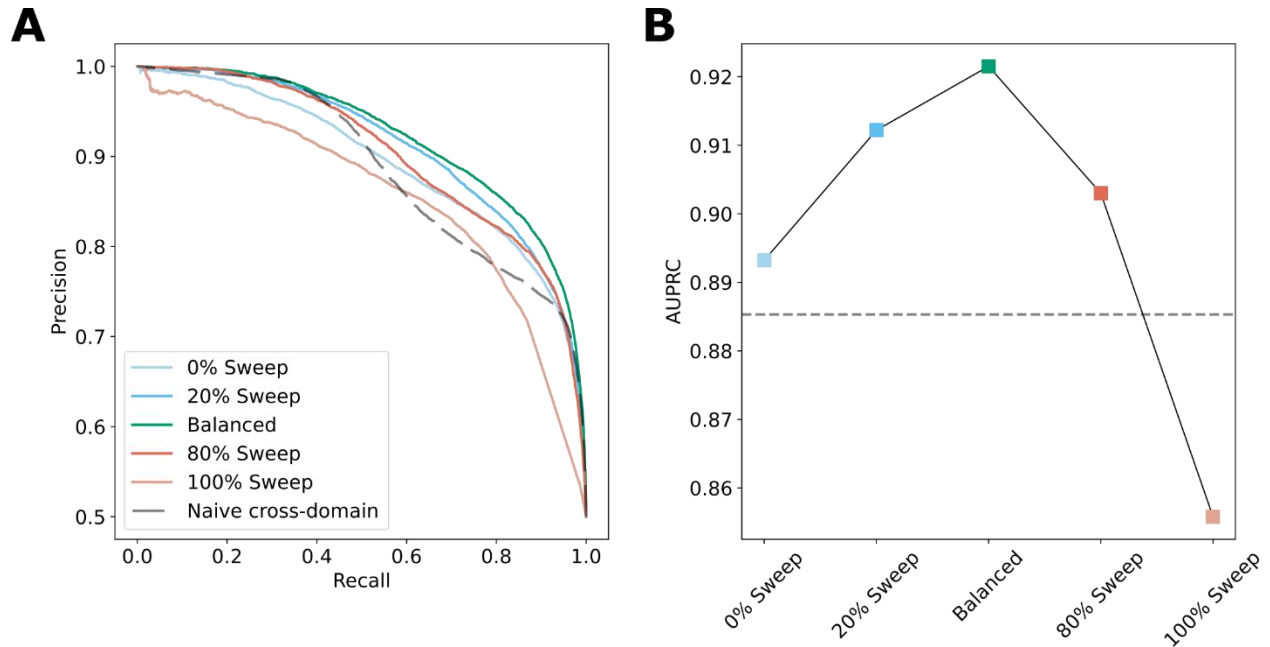
662 **Supplementary Figures**



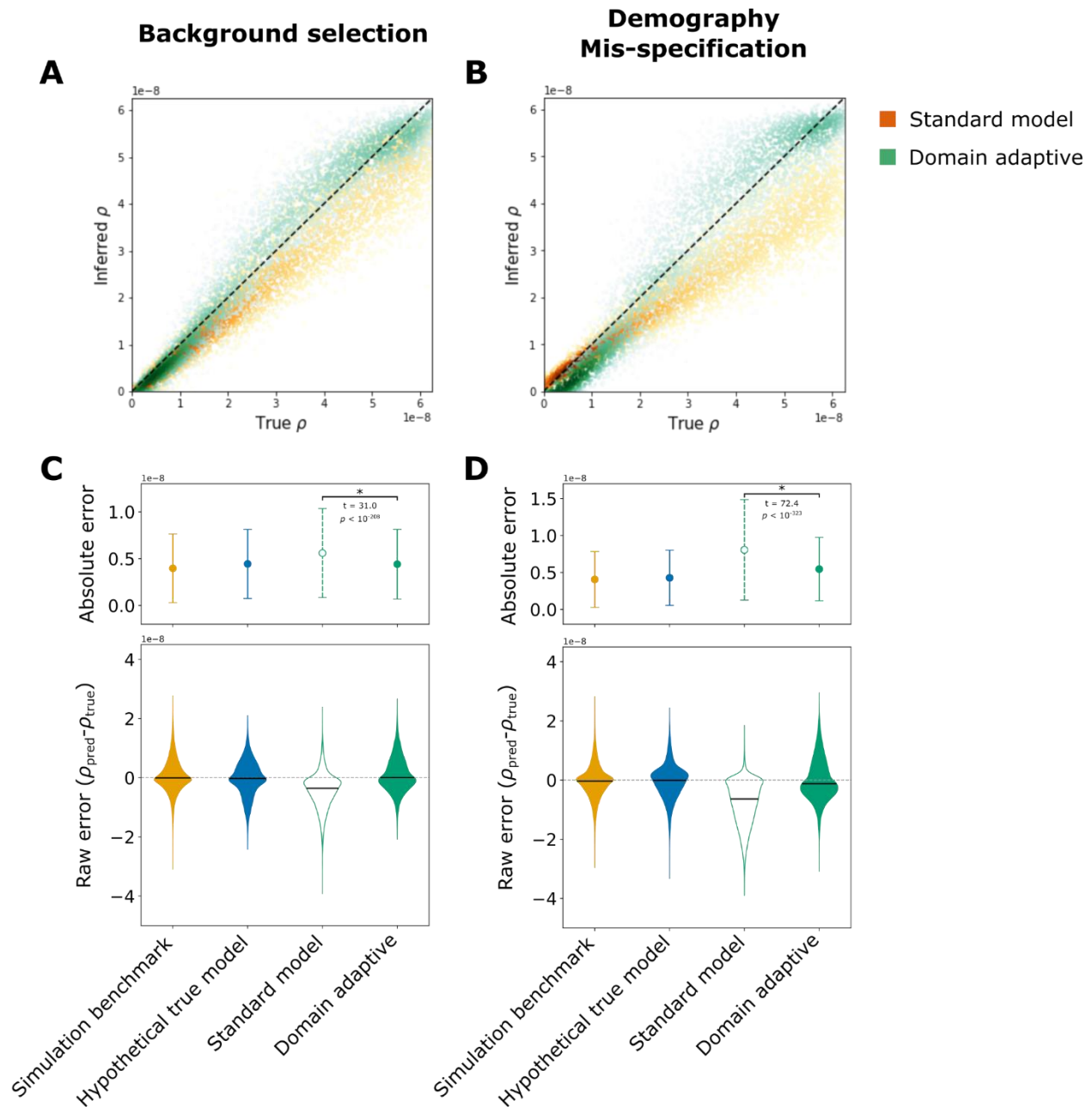
663 **Supplementary Figure 1. Domain-adaptive SIA. A)** The workflow of a simulation study
 664 that aims to benchmark the performance of the domain-adaptive SIA model in a realistic
 665 setting of demographic mis-specification. **B)** An improved version of SIA input features
 666 that encodes the full genealogy (adapted from (Kim et al. 2020)). A genealogy with n taxa
 667 at a polymorphic site is uniquely encoded by three $(n-1) \times (n-1)$ lower triangular matrices.
 668 The weight matrix W encodes the coalescent intervals where $w_{ij} = t_{n-j} - t_{n-1-i}, \forall i \geq j$,
 669 and the topology matrix F encodes the number of lineages persistent in the coalescent
 670 intervals corresponding to W (i.e. $f_{ij} = \#$ of lineages between t_{n-j} and $t_{n-1-i}, \forall i \geq j$). The
 671 derived lineage matrix R encodes only the subtree subtending the branch where the
 672 mutation occurred (red lightning symbol), following the same scheme as F . Note that the
 673 W matrix is a redundant encoding of the $n-1$ coalescent times $(t_1, t_2, \dots, t_{n-1})$, which contains
 674 information roughly equivalent to the original SIA ARG features (Hejase et al. 2022).



675 **Supplementary Figure 2. Selection coefficient inference performance of SIA**
 676 **models.** Raw data used to plot **Figs. 3B** and **3D** are presented in **(A)** and **(B)**,
 677 respectively. Performance of SIA models in the simulation experiment of failure to account
 678 for background selection **(C)** and in the simulation experiment of demographic model mis-
 679 specification **(D)** is presented in terms of mean and standard deviation of the absolute
 680 error (top) as well as the distribution of raw error (bottom). Statistical significance (*) of
 681 the difference between the absolute error of the standard model and that of the domain-
 682 adaptive model is evaluated with Welch's t -test. See **Fig. 1C** for definition of the model
 683 labels.



684 **Supplementary Figure 3. Sweep classification performance of domain-adaptive SIA**
 685 **models trained with imbalanced target domain data.** The classification performance
 686 of domain-adaptive SIA models trained with different proportions of sweep vs. neutral
 687 examples in the target domain is shown in the form of precision-recall curves (**A**) and the
 688 value of the area under precision-recall curve (AUPRC) (**B**). The dashed line in (**B**)
 689 indicates AUPRC of the standard model.



690 **Supplementary Figure 4. Recombination rate inference performance of ReLERNN**
 691 **models.** Raw data used to plot **Figs. 4A** and **4B** are presented in **(A)** and **(B)**,
 692 respectively. Performance of ReLERNN models in the simulation experiment of failure to
 693 account for background selection **(C)** and in the simulation experiment of demographic
 694 model mis-specification **(D)** is presented in terms of mean and standard deviation of the
 695 absolute error (top) as well as the distribution of raw error (bottom). Statistical significance
 696 (*) of the difference between the absolute error of the standard model and that of the
 697 domain-adaptive model is evaluated with Welch's *t*-test. See **Fig. 1C** for definition of the
 698 model labels.